Mechanical characterization and static validation of a satellite honeycomb sandwich structure

Ali Aborehab[a*], Mohammed Kassem[a], Ahmed Farid Nemnem[a] and M. Kamel[a]

[a]Aircraft Mechanics Departement, Military Technical College, Cairo, Egypt

ARTICLE INFO	ABSTRACT
	The honeycomb sandwich structures are extensively utilized in the satellite load bearing structure due to their superior mechanical properties. Investigating such structures and establishing their failure map implies the estimation of their equivalent elastic parameters as well as the experimental measurements of their ultimate strengths. Through a comprehensive study, this article discusses thoroughly the mechanical behavior of an aluminum honeycomb structure exposed to flat-wise compressive and flexural testing. Furthermore, an equivalent finite element model, based upon the sandwich theory, is proposed for simulating the elastic behavior of the flexural testing and comparing computational and experimental results. The comparison of results confirms accurately the usage of the sandwich theory and its related shell-volume-shell approach in the efficient modeling of honeycomb sandwich structures. In addition, the aforementioned honeycomb structure is parameterized from the geometry and material perspective. The outcome of such study reveals that the honeycomb core thickness has the greatest influence on the maximum displacement value. In addition, aluminum alloys are optimum choice for facing sheets material of the honeycomb structure.

1. Introduction

Honeycomb sandwich structures are composed of two thin facing sheets enclosing a light honeycomb core that is bonded to the facing sheets using structural adhesive (Zhang et al., 2016). Over the last decades, such structures have been employed in different structural applications including defensive armour, helicopter blades, marine structures, automotive industry, and satellites (Kolopp et al., 2013; Birman & Kardomateas, 2018; Vinson, 2005). They possess outstanding specific strength/stiffness, flexural rigidity, dimensional stability, and superior energy absorption. Thus, those structures have drawn the attention extensively in aerospace applications (Li et al., 2016; Aborehab et al., 2020). Finite element modeling (FEM) of honeycomb sandwich structures poses an extreme challenge, since detailed modeling is of a very high computational expense. Consequently, equivalent FEM of those structures is inescapable. It involves the estimation of the equivalent elastic properties of the honeycomb core or for the whole sandwich structure. However, these equivalent methods need to be validated with an experimental work. To date, many studies have been implemented concerning the equivalent modeling of sandwich structures (Xia et al., 2001; Hao et al., 2011; Boudjemai et al., 2012; Jiang et al., 2014; Fu et al., 2017; Sun & Cheng, 2017). Xia et al. (2001) proposed three equivalent modeling theories, namely

* Corresponding author.
E-mail addresses: ali.aborehab@gmail.com (A. Aborehab)

sandwich theory, equivalent plate theory, and honeycomb plate theory. They concluded the reliability of such theories in the modeling process of sandwich structures. Boudjemai et al. (2012) concentrated on the equivalent plate theory and proved the consistency of such theory numerical results when compared to experimental results. Meanwhile, Jiang et al. (2014) utilized the three-layered sandwich theory in the efficient calculation of elastic properties and validated the usage of such theory by conducting an experimental modal testing and comparing both computational and experimental results.

Nevertheless, computing the equivalent elastic properties is not sufficient for full mechanical characterization of honeycomb structures. Investigating such structures and predicting their failure modes map require measuring their mechanical properties using experimental work. Over the past decades, a great number of studies were carried out for the sake of measuring the ultimate compressive and shear strengths of the investigated honeycomb core (Khan, 2006; Feraboli, 2006; Bianchi et al., 2010; Kim & Lee, 2010; Cheng et al., 2015; Ashab et al., 2016; Liu et al., 2017). Khan (2006) implemented flat-wise compressive tests on honeycomb sandwich panels with different facing sheets material and different core thickness. The study investigated the out-of-plane compressive strength and ensured the great influence of facing sheets material on the compressive strength rather than the secondary effect of core thickness. Cheng et al. (2015) carried out a compression testing on aluminum honeycomb sandwich panels with different structural adhesive layer thicknesses. They concluded that the energy absorption of honeycomb panels decreased with the increase of adhesive layer thickness. Liu et al. (2017) investigated the compressive properties of Nomex honeycomb core sandwich structure with different core thicknesses. They performed a detailed FEM (mesoscopic model) of the structure under investigation using ABAQUS/Explicit software and concluded that increasing the core thickness decreases the ultimate compressive strength and vice versa.

Other experimental crucial studies were carried out to investigate the flexural behavior of honeycomb structures and the associated failure modes (Zhang et al., 2016; Sun et al., 2017; Czechowski et al., 2017; Lv et al., 2018; Hussain et al., 2018; Su et al., 2018; Rodriguez-Ramirez et al., 2018). Sun et al. (2017) discussed the mechanical behavior of aluminum honeycomb panels subjected to three-point bending and in-plane compression loads. They conducted a parametric study taking into consideration the panel geometric effects. Moreover, they constructed a detailed (full-scale) FEM to be validated with experimental results. They achieved a good agreement between computational and experimental results. Lv et al. (2018) fabricated honeycomb sandwich panels with three different core cross-sections and tested their bending properties via three-point bending test. They assumed that the hexagonal cross section acquired the maximum loading, whereas; the triquetrous had the lowest. Hussain et al. (2018) investigated honeycomb sandwich beams, of fiber glass facing sheets and aluminum honeycomb core, experimentally and numerically. They predicted failure modes concerning static and fatigue loadings. Recently, Rodriguez-Ramirez et al. (2018) conducted a study on the shear behavior of a honeycomb sandwich beam experimentally and numerically. Three-point bending tests were implemented in order to investigate the shear buckling of core and it was concluded that such buckling was severely affected by boundary conditions.

Despite these aforementioned researches, to the author's foremost information, the researches on investigating and validating aluminum honeycomb sandwich structures remain quite insufficient so far. This article aims to provide more investigations on space-qualified honeycomb structures response through experimental and numerical work. The article is organized as follows. Firstly, flat-wise compressive testing (bare and stabilized) is implemented according to ASTM standard C-365 (C365-00, 2000) and results are compared with the published data of the widely used honeycomb company (HEXCEL-Composites, HexWeb Honeycomb Attributes and Properties, 1999). Subsequently, three-point bending tests are carried out on honeycomb sandwich beams in both L and W orientations according to ASTM standard C-393 (C393-00, 2000). Meanwhile, a FEM is performed to simulate the aforementioned test using static analysis module in ANSYS which validates the equivalent modeling theory (sandwich theory) and its related approach. Finally, a parametric study is executed to relate the static analysis results with several aspects including material and geometrical variations.

2. Flat-wise compressive testing of honeycomb core

2.1 Test Scope and Testing Machine

This test is performed according to the ASTM standard C-365 (C365-00, 2000) for the sake of determining the ultimate compressive strength of honeycomb sandwich core. The ultimate compressive strength is measured in the direction normal to the plane of facing sheets. Another purpose of the test is to investigate the difference between the ultimate compressive strength for both bare and stabilized specimens.

The apparatus used to perform this test is "H100KU" which belongs to the American company "Tinius Olsen" (Olsen, 2010). This machine has a frame capacity of 100 kN and it provides load measurement accuracy of ±0.5% of the applied load. The testing machine is equipped with a remote control panel with an LCD display, it serves to move the cross bar, display the load, position, speed of movement of the cross bar and deformation of the sample. The machine is provided with special grips that are dedicated for compressive testing.

2.2 Test Specimens

Compressive testing comprises two types according to the shape of test specimens as follows:

1. Bare compressive test: when the test is implemented on the honeycomb core cells without facing sheets.

2. Stabilized compressive test: when the test is implemented on a honeycomb core that is reinforced with a thin layer of resin or thin facing sheets bonded to the core.

In this research, both aforementioned compressive testing are implemented utilizing three test specimens for each test. The dimensions of the specimens are selected according to ASTM standard C-365 (C365-00, 2000). The specimens are of square shape of 60 mm side length and 8 mm thickness. The utilized honeycomb is space-qualified, perforated, and regular hexagon core of designation 1/8 – AL 5052 – 0.002 (P). The geometric properties of the utilized honeycomb core are shown in Fig. 1. For stabilized testing, the aforementioned honeycomb core is bonded to two upper and lower aluminum facing sheets AL 7075-T6 of thickness 1.5 mm (total sandwich thickness is 11 mm).
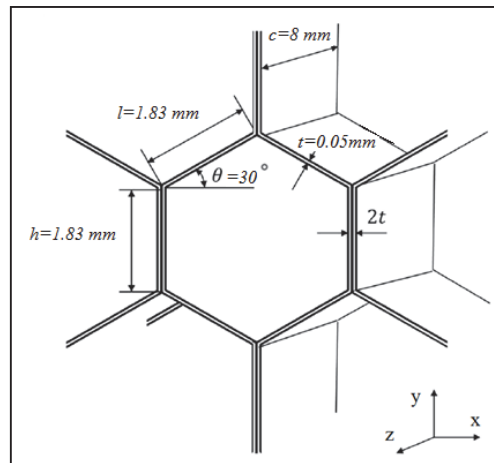

Fig. 1. Geometric properties of utilized honeycomb core

2.3 Test Procedure

The load is applied to the specimen using cylindrical blocks which distribute the load uniformly over the entire surface of the specimen. It should be taken into consideration to load the specimen ends uniformly and parallel to the loading surfaces. The load is applied at a constant rate of movement of the testing machine cross-head (0.5 mm/min), such that the maximum load will occur between 3 and 6

minutes. The load-deflection curves are determined, and the flat-wise ultimate compressive strength is calculated as follows:

$$\sigma = \frac{P}{A},$$ (1)

where σ is the ultimate compressive strength, MPa; P is the ultimate load, N; A is the cross-sectional area, mm^2. Fig. 2 depicts the setup of flat-wise compressive testing of the honeycomb sandwich structure under investigation.
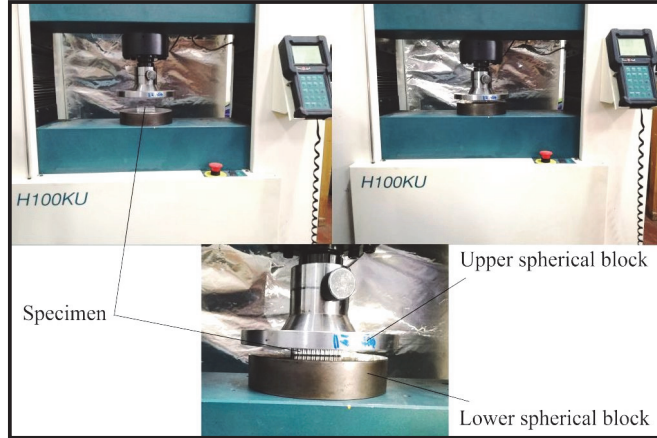

Fig. 2. Compressive testing setup

2.4 Test Results

The results of bare compressive testing, compared with the published results (HEXCEL-Composites, HexWeb Honeycomb Attributes and Properties, 1999), are highlighted in Table 1 and Fig. 3. The deviation of ultimate compressive strength is calculated as follows:

$$Deviation = \frac{|Referenced\ strength - Mean\ measured\ strength|}{Referenced\ strength} \times 100\%$$ (2)

Table 1. Bare compressive testing results.

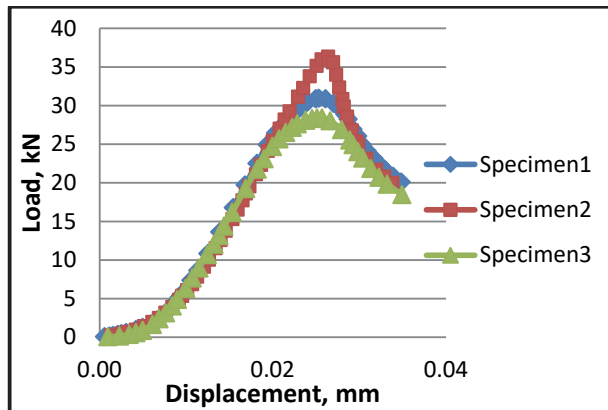| Specimen no.	Ultimate strength, MPa (HEXCEL-Composites, HexWeb Honeycomb Attributes and Properties, 1999)	Ultimate load, kN	Ultimate strength, MPa	Mean, MPa	Deviation, %
Specimen 1		31.2	8.7		
Specimen 2	10.34	36.5	10.14	8.93	13.64
Specimen 3		28.6	7.94		

Fig. 3. Load-displacement curve of bare specimens

The results of the stabilized compressive testing, compared with the published results (HEXCEL-Composites, HexWeb Honeycomb Attributes and Properties, 1999), are shown in Table 2 and Fig. 4. Fig. 5 depicts two samples of the compressive test specimens after carrying out the test.

Table 2. Stabilized compressive testing results

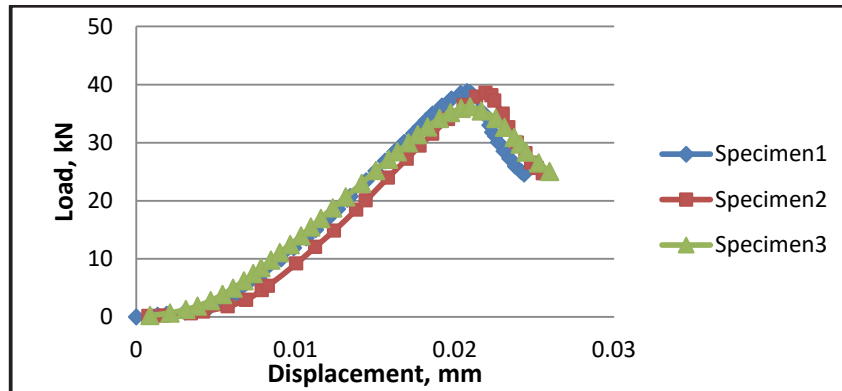| Specimen no.	Ultimate strength, MPa (HEXCEL-Composites, HexWeb Honeycomb Attributes and Properties, 1999)	Ultimate load, kN	Ultimate strength, MPa	Mean, MPa	Deviation, %
Specimen 1		38.8	10.78		
Specimen 2	10.76	38.6	10.72	10.52	2.23
Specimen 3		36.2	10.06		

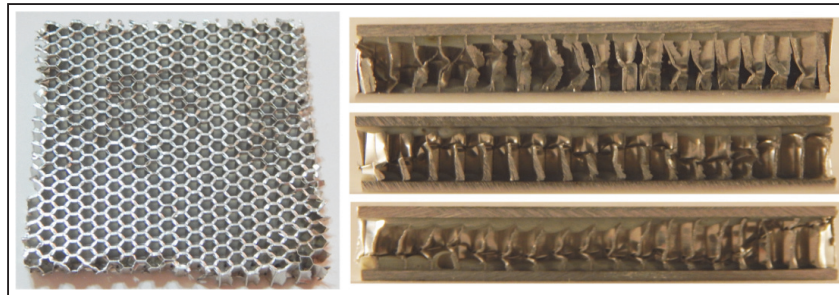**Fig. 4.** Load-displacement curve of stabilized specimens

Fig. 5. Samples of the compressive test specimens after carrying out the test

Based upon the aforementioned results, it can be deduced that both bare and stabilized flat-wise compressive testing are carried out successfully. The measured results of the ultimate compressive load and the related ultimate compressive strength are in a good agreement with the published experimental results (HEXCEL-Composites, HexWeb Honeycomb Attributes and Properties, 1999). However, stabilized specimens show better agreement than bare ones as the usage of two facing sheets bonded to the core (stabilized specimens) helps in avoiding the local crushing at the ends of some honeycomb core cells. This can result in an obvious increment in the ultimate compressive strength of the stabilized specimens compared with the bare ones.

3. Flexible testing of honeycomb sandwich structure

Flexural testing includes either single-point load (three-point bending) or two-point load (four-point bending). In this research, three-point bending is utilized to calculate flexural properties.

3.1 Test Scope and Testing Machine

This test is carried out according to the ASTM standard C-393 (C393-00, 2000) with the sake of determining the ultimate shear strength of honeycomb sandwich core in both L and W directions shown

in Fig. 6. Another purpose of this test is to validate the approach used in the research for modeling honeycomb sandwich structures. The validation is implemented by measuring the deflection values at different applied loads in the elastic zone and comparing such values with the numerical values of the deflection calculated at the same loads while simulating the above-mentioned test using static analysis module in ANSYS workbench.
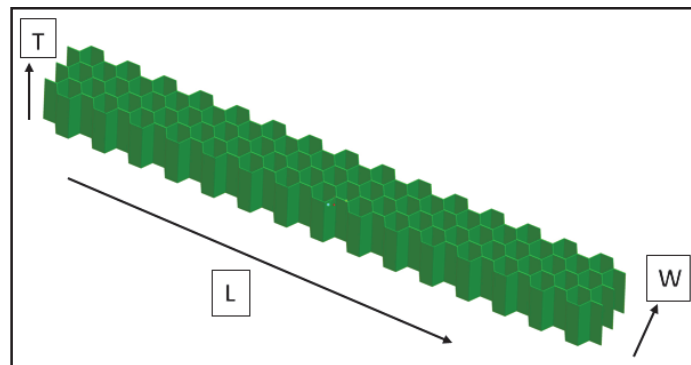

Fig. 6. Honeycomb core directions

The testing machine used to perform this test is "Z010" which belongs to the German company "Zwick Roell" (Roell, 2018). Such type of machines is universal, designed to implement miscellaneous static tests. This machine has a load frame of 10 kN with force measurement accuracy of ±0.5% of the applied load. The testing machine is equipped with special grips designed for three-point testing.

3.2 Test Specimens

Test specimens shall be of rectangular shape (beam shape) as mentioned in ASTM standard C-393 (C393-00, 2000). The specimens comprise two sets that are manufactured such that the test can be conducted in the two principle orientations of honeycomb core: the L and W orientations. L-oriented specimens are prepared such that the honeycomb core L-direction is oriented along the specimen length direction. Similarly, W-oriented specimens are prepared. Each set includes three specimens. The six specimens are prepared with 140 mm length, 100 mm span length, 25 mm width, and 11 mm thickness represented in 8 mm for the core and 1.5 mm for each facing sheet as shown in Fig. 7. Aluminum facing sheets AL 7075-T6 are utilized. The geometric, physical, and mechanical properties of the utilized honeycomb core are similar to the specifications used in the previously mentioned compressive testing as introduced in subsection 2.2.
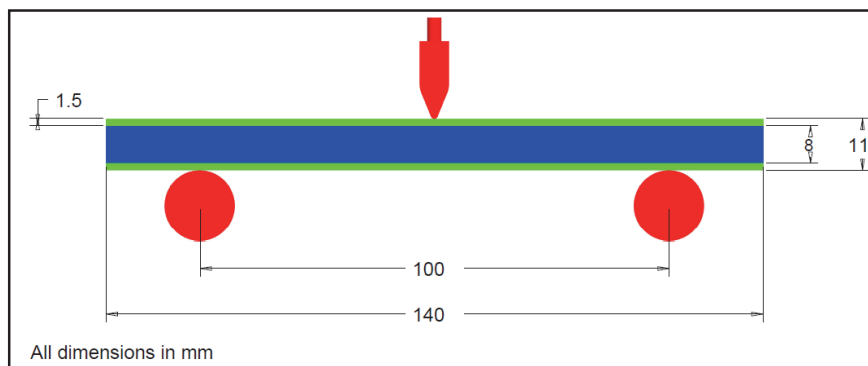

Fig. 7. Three-point bending test scheme

3.3 Test Procedure

The load is applied to the specimen through a steel loading bar, in such a way that the loading bar is positioned in the middle of the specimens span length on their upper surface. The specimens are supported on two roller bars, which allow free rotation as shown in Fig. 8. The load is applied at a constant rate of movement of the testing machine cross-head (1 mm/min), such that the maximum load

will occur between 3 and 6 minutes. The load-deflection curves are determined, and the core ultimate shear strengths are calculated as follows:

$$\tau = \frac{P}{(d + c) * b} \tag{3}$$

where: τ is the ultimate shear strength, MPa; P is the ultimate load, N; d is the honeycomb sandwich thickness, mm; c is the honeycomb core thickness, mm; and b is the honeycomb sandwich width, mm.

Fig. 8. Three-point bending test setup

3.4 Test Results

The results of three-point bending test for L-oriented specimens, compared with the published results (HEXCEL-Composites, HexWeb Honeycomb Attributes and Properties, 1999), are presented in Table 3. Fig. 9 introduces the load-displacement curves of the three specimens; each curve includes approximately 3800 measured points that are received from the testing machine.

Table 3. Three-point bending test results for L-oriented specimens

Specimen no.	Ultimate strength, MPa (HEXCEL-Composites, HexWeb Honeycomb Attributes and Properties, 1999)	Ultimate load, N	Ultimate strength, MPa	Mean, MPa	Deviation, %
Specimen 1		2860.64	6.02		
Specimen 2	6.3	2824.94	5.95	5.92	6.03
Specimen 3		2752.35	5.79		

The results of three-point bending test for W-oriented specimens, compared with the published results of (HEXCEL-Composites, HexWeb Honeycomb Attributes and Properties, 1999), are listed in Table 4 and Fig. 10 introduces the load-displacement curves of the three specimens; each curve includes approximately 4200 measured points that are received from the testing machine.
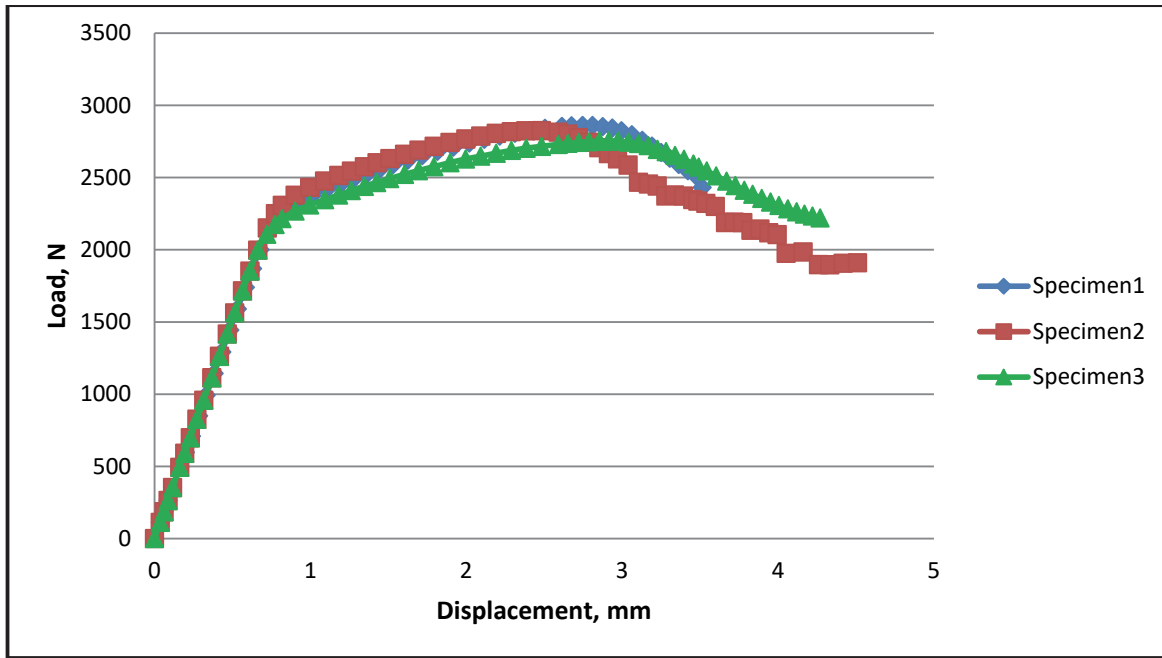
Fig. 9. Load-Displacement curve for L-oriented specimens

Table 4. Three-point bending test results for W-oriented specimens

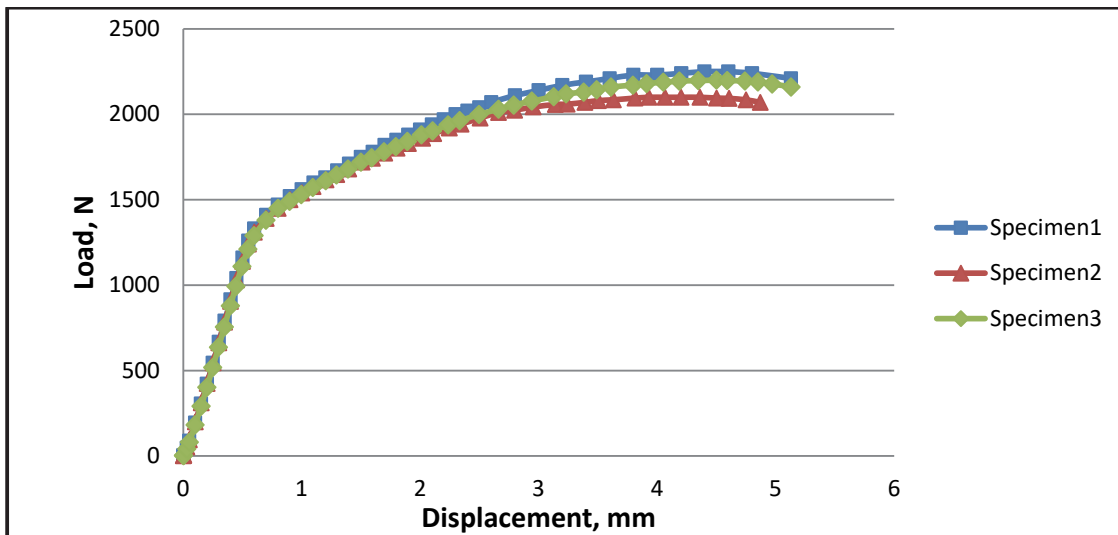| Specimen no.	Ultimate strength, MPa (HEXCEL-Composites, HexWeb Honeycomb Attributes and Properties, 1999)	Ultimate load, N	Ultimate strength, MPa	Mean, MPa	Deviation, %
Specimen 1		2250	4.74		
Specimen 2	4.82	2100	4.42	4.59	4.77
Specimen 3		2198.76	4.63		

Fig. 10. Load-Displacement curve for W-oriented specimens

The load-displacement curves for both L-oriented and W-oriented specimens introduce clearly the elastic zones, plastic zones, failure points, and ultimate shear strengths. The linear elastic zone for L-oriented specimens ends approximately at a mean load value of 2000 N, whereas it ends nearly at 1200 N for W-oriented specimens. The ultimate shear strength occurs at a mean load value of 2800 N for L-oriented specimens, while it occurs at 2200 N for W-oriented specimens. These values agree in concept

with the fact that the L-direction is the strongest and the stiffest direction and the W-direction is the most compliant. Fig. 11 depicts two samples of the three-point bending specimens after carrying out the aforesaid test.
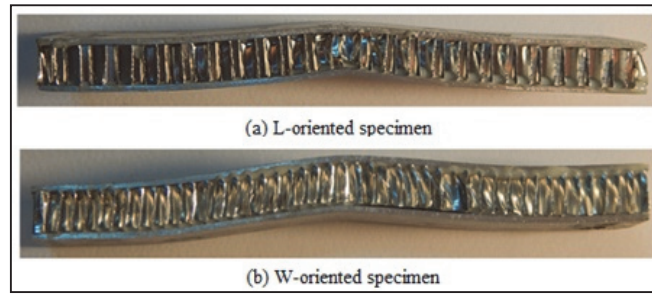

(a) L-oriented specimen

(b) W-oriented specimen

Fig. 11. Samples of the three-point bending test specimens after carrying out the test

Based upon the mentioned results, it can be deduced that three-point bending tests in both L & W directions are carried out successfully. The measured results of the ultimate shear strengths in both directions are in a good agreement with the published experimental results (HEXCEL-Composites, HexWeb Honeycomb Attributes and Properties, 1999). The subsequent step is to validate the approach used in the research for modeling honeycomb sandwich structures by simulating the aforementioned test using FEM via static analysis module in ANSYS workbench.

4. FEM of honeycomb sandwich specimens

In this article, sandwich theory has been selected as an equivalent theory for FEM of honeycomb structures. In order to validate the proposed equivalent model, the aforementioned three-point bending test is modeled and simulated using static analysis module in ANSYS workbench. Results of both numerical and experimental work are compared in the linear elastic zone.

4.1 Sandwich Theory

The sandwich theory represents definitely the layered nature of honeycomb sandwich structures. For such theory, the honeycomb core is dealt with as a homogenized continuum with orthotropic specifications. Thus, the main requirement of sandwich theory is to estimate accurately the equivalent elastic properties of the homogenized core with double thickness walls. Such properties depends extensively on the mechanical properties of the honeycomb core material (E_c, G_c, and v_c) plus the geometric properties of the core unit cell represented in vertical wall length h, inclined wall length l, inclined wall thickness t, cell angle θ, and core thickness c as shown in Fig. 1.

The equivalent properties include in-plane and out-of-plane equivalent elastic properties. The in-plane properties include four elastic properties; two moduli of elasticity (E_x, E_y), shear modulus (G_{xy}), and Poisson's ratio (v_{xy}). They are calculated according to (Gibson & Ashby, 1997) and (Sorohan et al., 2015).

$$E_x = \left(\frac{t}{l}\right)^3 \frac{\cos\theta}{\sin^2\theta \left(\frac{h}{l} + \sin\theta\right)} E_c \qquad (4)$$

$$E_y = \left(\frac{t}{l}\right)^3 \frac{\left(\frac{h}{l} + \sin\theta\right)}{\cos^3\theta} E_c \qquad (5)$$

$$G_{xy} = \left(\frac{t}{l}\right)^3 \frac{\left(\frac{h}{l} + \sin\theta\right)}{\left(\frac{h}{l}\right)^2 \left(1 + \frac{h}{4l}\right)\cos\theta} E_c \qquad (6)$$

$$v_{xy} = \frac{\cos^2\theta}{\sin\theta \left(\frac{h}{l} + \sin\theta\right)} \approx 1 \qquad (7)$$

The out-of-plane equivalent elastic properties include five elastic moduli; modulus of elasticity (E_z), shear moduli (G_{xz}, G_{yz}), and two Poisson's ratios (v_{xz}, v_{yz}). The modulus of elasticity (E_z) is estimated as follows (Gibson & Ashby, 1997):

$$E_z = \left(\frac{t}{l}\right)\frac{\left(\frac{h}{l}+1\right)}{\cos\theta\left(\frac{h}{l}+\sin\theta\right)} E_c \tag{8}$$

The two Poisson's ratios (v_{xy}) and (v_{zy}) are calculated as follows:

$$v_{xy} = \frac{E_x}{E_y}v_c \approx 0, v_{zy} = \frac{E_z}{E_y}v_c \approx 0 \tag{9}$$

The calculation of shear moduli is more complex and exact calculations are not possible. Nonetheless, upper and lower bounds for such moduli can be formulated using the published method (Kelsey et al., 1958). For the shear modulus (G_{xz}), both bounds coincide as follows:

$$G_{xz} = \frac{\cos\theta}{\left(\frac{h}{l}+\sin\theta\right)}\left(\frac{t}{l}\right)G_c \tag{10}$$

For the shear modulus (G_{yz}), both bounds do not coincide as follows (Kelsey et al., 1958):

$$\left(\frac{t}{l}\right)\frac{\left(\frac{h}{l}+\sin\theta\right)}{\cos\theta\left(1+\frac{h}{l}\right)} G_c \leq G_{yz} \leq \left(\frac{t}{l}\right)\frac{\left(\frac{h}{l}+\sin^2\theta\right)}{\cos\theta\left(\frac{h}{l}+\sin\theta\right)} G_c \tag{11}$$

Grediac (1993) proposed a formula for calculating (G_{yz}) based upon finite element analysis; it depends upon core thickness (c) to wall length (l) ratios as follows:

$$G_{yz} = G_{yz}{}^{low.} + \frac{0.787}{\left(c/l\right)}\left(G_{yz}{}^{upp.} - G_{yz}{}^{low.}\right) \tag{12}$$

4.2 Static Analysis of Honeycomb Sandwich Structure

The honeycomb sandwich beams are modeled in ANSYS workbench according to the sandwich theory using shell-volume-shell approach (SVS), where the upper and lower facing sheets are modeled using shell finite elements "shell 181", while the core volume is modeled via solid finite elements "solid 186". The properties of the core material (AL-5052) are presented in Table 5.

Table 5. Material properties of core material

E_c	ρ_c	v_c
70 GPa	2700 kg/m³	0.33

The honeycomb core equivalent elastic parameters are calculated using the above-mentioned formulas. The mechanical and physical properties of facing sheets and core are shown in Table 6 and Table 7, respectively.

Table 6. Material properties of the facing sheets

E	ρ_f	v
70 GPa	2800 kg/m³	0.33

Table 7. Equivalent material properties of the honeycomb core

E_x	3.3 MPa	E_z	2944.6 MPa
E_y	3.3 MPa	G_{xz}	426 MPa
G_{xy}	1.98 MPa	G_{yz}	651.7 MPa
v_{xy}	1	v_{xz}	0
v_{yz}	0	$\rho_{eq.}$	130 kg/m³

The three-point bending tests in L and W directions are simulated using static analysis module. The simulation is implemented four times at different applied loads. For L-orientation, the simulation is carried out at 500 N, 1000 N, 1500 N, and 2000 N. For W-orientation, the simulation is carried out at 250 N, 500 N, 750 N, and 1000 N. Meshing is carried out using fine mesh with element size 1.5 mm, at which results converge as shown in Fig. 12 and 13. Table 8 lists the total number of elements and nodes used for meshing the FEM.

Table 8. Number of elements and nodes used to mesh the honeycomb sandwich beam

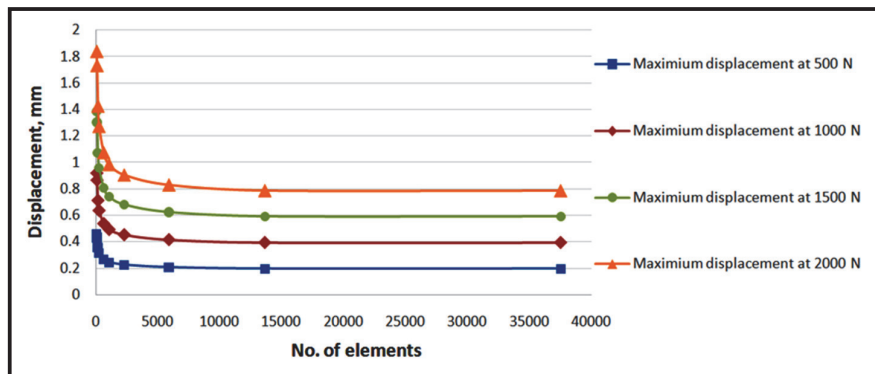| Element size, mm	Number of elements	Number of nodes
1.5	13617	51907

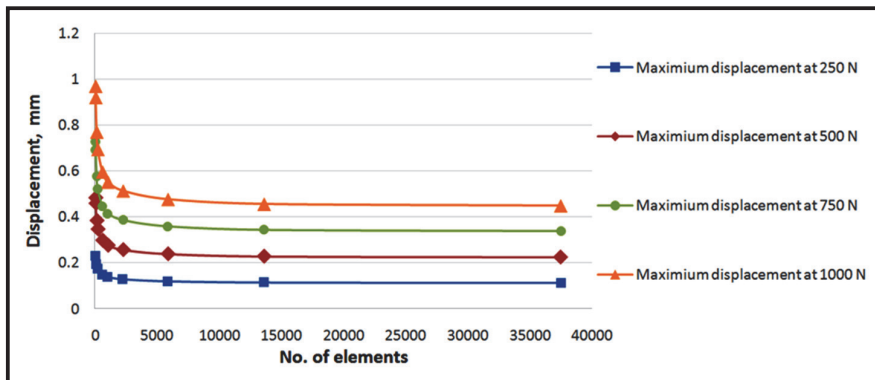**Fig. 12.** Mesh sensitivity analysis of L-oriented beams.

Fig. 13. Mesh sensitivity analysis of W-oriented beams.

4.3 Results Comparison and Discussion

The results comparison between both experimental three-point bending tests and numerical static analysis for L-oriented specimens are shown in Table 9.

Table 9. Experimental and numerical results comparison (L-direction)

Load	Displacement, mm				
	Spec. 1	Spec. 2	Spec. 3	Mean value	Numerical value
500	0.16445	0.1641165	0.1641175	0.164228	0.16855
1000	0.333808	0.329736	0.3298969	0.331147	0.3371
1500	0.501765	0.4939577	0.4944836	0.496735	0.50565
2000	0.6765	0.6622	0.66401	0.66757	0.6742
Mean deviation %					1.81

Based upon the aforesaid data, it can be denoted that there is a close matching between the experimental three-point bending tests and the static numerical analysis concerning the L-oriented specimens; the mean deviation does not exceed 1.81 %. Table 10 and Fig. 15 introduce the results

comparison between both experimental three-point bending tests and numerical static analysis for W-oriented specimens.   The deviation of displacement at each applied load value is calculated as follows:

$$Deviation = \frac{|displacement_{num} - displacement_{exp}|}{displacement_{exp}} \times 100\% \qquad (13)$$
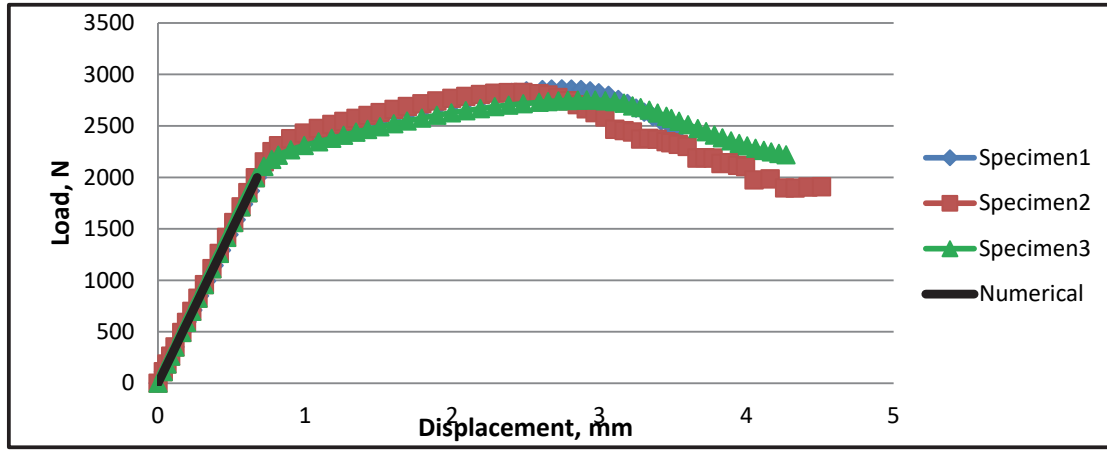

Fig. 14. Experimental and numerical results comparison (L-orientation).

Based upon the aforesaid data, it can be denoted that there is a close matching between the experimental three-point bending tests and the static numerical analysis concerning the L-oriented specimens; the mean deviation does not exceed 1.81 %. Table 10 and Fig. 15 introduce the results comparison between both experimental three-point bending tests and numerical static analysis for W-oriented specimens. It can be observed that the numerical results are in close agreement with the experimental results; the mean deviation does not exceed 2.21 % in both directions. Fig. 16 and 17 show samples from the calculated displacement using static analysis module in ANSYS workbench concerning L-oriented and W-oriented specimens respectively. It is clear that the maximum displacement occurs definitely at the mid-span distance for all specimens.
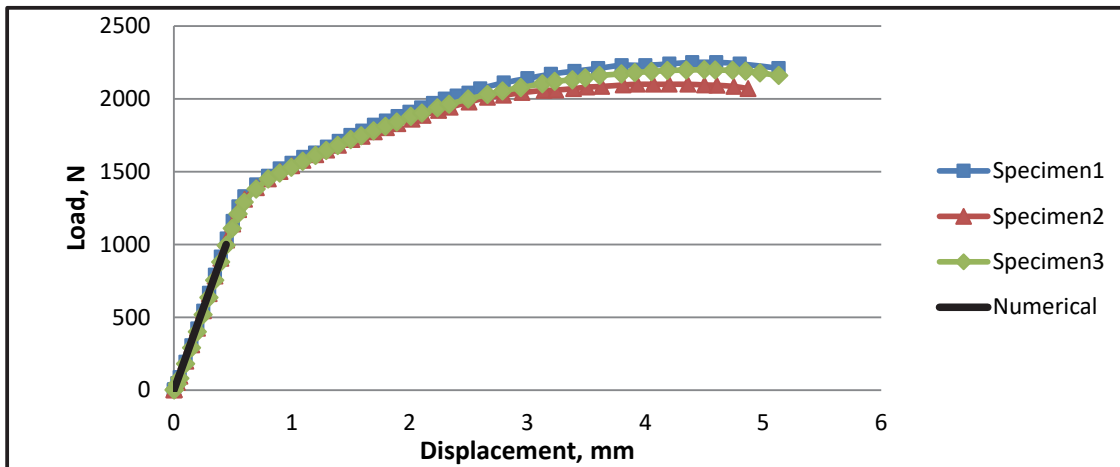

Fig. 15. Experimental and numerical results comparison (W-orientation)
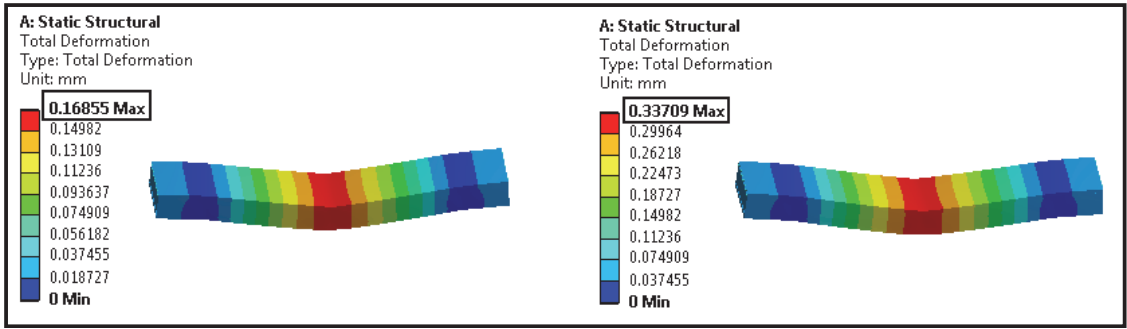
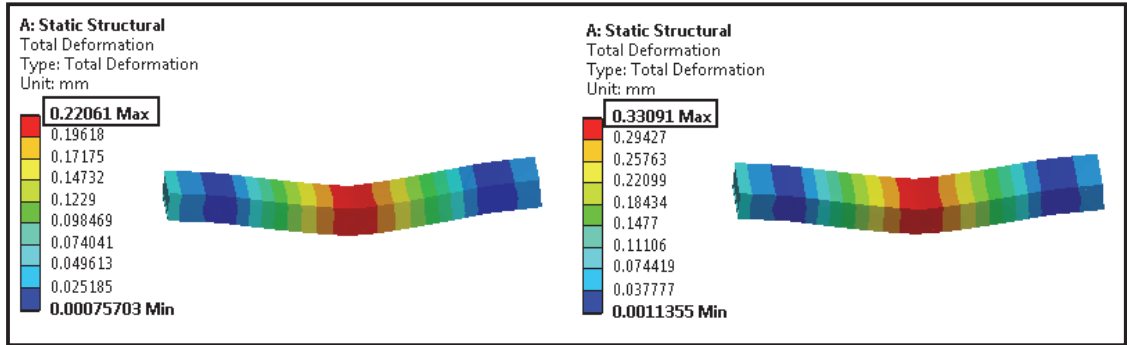**Fig. 16.** FEM results of L-oriented specimens

Fig. 17. FEM results of W-oriented specimens

5. Honeycomb sandwich beam parametric study

This study is implemented in order to find the influence of several parameters including the honeycomb core thickness, facing sheets thickness, and facing sheets material on the maximum displacement that occurs during the simulation of three-point bending test in both orientations.

5.1 Influence of Honeycomb Core and Facing Sheets Thicknesses

Static analysis is carried out upon the previously mentioned honeycomb sandwich beams with the following dimensions: 140 mm length, 100 mm span length, and 25 mm width. The honeycomb core thickness is allowed to vary from 8 mm up to 20 mm while permitting the facing sheets thickness to vary from 1.5 mm up to 1.22 mm such that the specimens' masses are kept constant. Fig. 18 illustrates the relation between the non-dimensional displacement (displacement/sandwich thickness) and the non-dimensional quantity representing (facing sheets thickness/core thickness) for both L-oriented and W-oriented specimens under 1000 N.
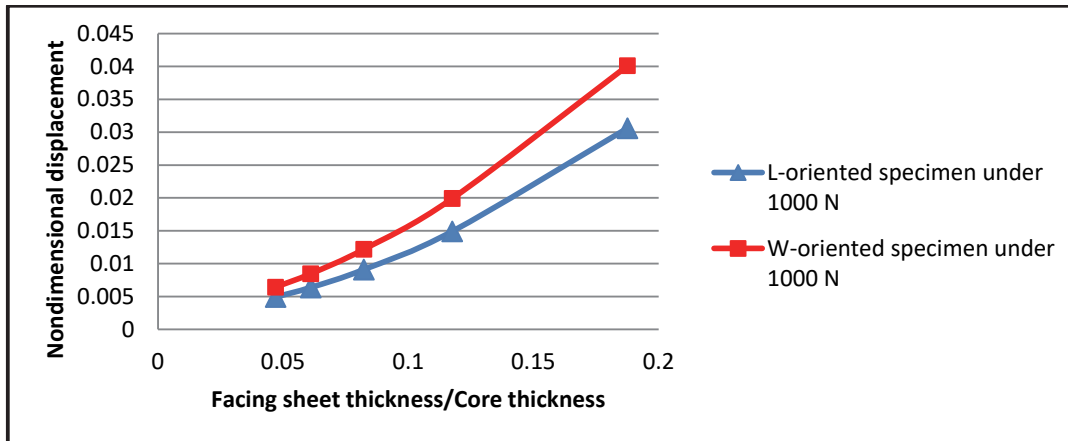

Fig. 18. Influence of core and facing sheets thicknesses on the non-dimensional maximum displacement

It is clear that regardless of the specimen orientation, increasing the non-dimensional quantity (facing sheets thickness/core thickness) leads to a significant increment in the non-dimensional maximum displacement value while maintaining constant specimens' masses. That's why, it can be concluded that the core thickness is more influential on the non-dimensional displacement than facing sheets thickness due to its superior specific stiffness.

5.2 Influence of Facing Sheets Material

Static analysis is executed on the honeycomb sandwich beam with the following dimensions: 140 mm length, 100 mm span length, 25 mm width, and 8 mm core thickness. Three miscellaneous isotropic alloys are used for facing sheets; each alloy is related to a facing sheet thickness such that the specimens' masses are kept constant as shown in Table 11.

Table 11. Material properties of the used alloys

Alloy Type	E, GPa	ρ_f, kg/m^3	υ	Facing sheets thickness, mm
AL7075-T6	70	2800	0.33	1.5
Ti-6AL-4V	110	4500	0.33	0.935
Steel 4340	200	7800	0.3	0.54

Fig. 19 depicts the influence of the facing sheets material variation on the non-dimensional displacement of the honeycomb sandwich beam for both L-oriented and W-oriented specimens under 1000 N.
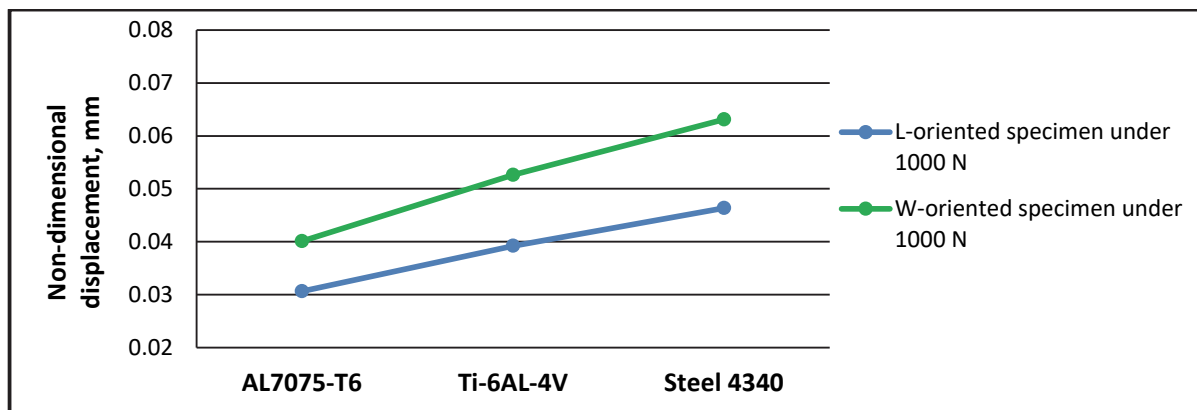

Fig. 19. Influence of facing sheets thickness on natural frequency

It can be deduced that the facing sheets material variation has a crucial influence on the non-dimensional displacement value. While maintaining constant specimens' masses, aluminum alloys are considered the optimum metallic materials for the facing sheets due to their considerable specific stiffness.

6. Conclusions

Bare and stabilized flat-wise compressive testing is implemented according to ASTM standard C-365 and the maximum compressive strength is measured and compared to the published results of "HEXCEL Composites" company, acceptable deviation is received. However, stabilized specimens show better agreement (2.23%) than bare ones (13.64%) as the usage of two facing sheets bonded to the core helps in avoiding the local crushing at the ends of some honeycomb core cells. This can result in an obvious increment in the ultimate compressive strength of the stabilized specimens compared with the bare ones. Concurrently, three-point bending tests are carried out on honeycomb sandwich beams in both L and W orientations according to ASTM standard C-393. The ultimate shear strengths in both L and W orientations are measured and compared to the published data of "HEXCEL Composites" company, good agreement is received; the mean deviation does not exceed 6%. Meanwhile, the three-point bending tests results are utilized to validate an equivalent FEM based upon the sandwich theory and its related shell-

volume-shell (SVS) approach. Experimental and computational results comparison shows a close matching; the mean deviation does not exceed 2.21%. Finally, the parametric study results assure that the honeycomb core thickness is the most influential parameter on the non-dimensional maximum displacement value during three-point bending test simulation on ANSYS workbench software. Besides, aluminum alloys are regarded as an optimum choice for facing sheets material.

References

Aborehab, A., Kassem, M., Nemnem, A. F., Kamel, M., & Kamel, H. (2020). Configuration design and modeling of an efficient small satellite structure. *Engineering Solid Mechanics , 8* (1), 7-20.

Ashab, A., Ruan, D., Lu, G., & Bhuiyan, A. A. (2016). Finite Element Analysis of Aluminum Honeycombs Subjected to Dynamic Indentation and Compression Loads. *Materials , 9* (3).

Bianchi, G., Aglietti, G. S., & Richardson, G. (2010). Development of Efficient and Cost-Effective Spacecraft Structures Based on Honeycomb Panel Assemblies. *IEEE Aerospace Conference.*

Birman, V., & Kardomateas, G. (2018). Review of current trends in research and applications of sandwich structures. *Composites Part B , 142*, 221-240.

Boudjemai, A., Amri, R., Mankour, A., Salem, H., Bouanane, M., & Boutchicha, D. (2012). Modal analysis and testing of hexagonal honeycomb plates used for satellite structural design. *Materials and Design , 35*, 266–275.

C365-00. (2000, April). Standard Test Method for Flatwise Compressive Properties of Sandwich Cores. *ASTM* .

C393-00. (2000). Standard Test Method for Flexural Properties of Sandwich Constructions. *ASTM* .

Cheng, S., Zhao, B., Xiao, Z., & Xin, Y. (2015). Compression tests on aluminum honeycomband epoxy resin sandwich panels. *Emerging Materials Research , 4* (EMR2).

Czechowski, L., Jankowski, J., & Kotełko, M. (2017). Experimental and numerical three-point bending test for sandwich beams. *Journal of KONES Powertrain and Transport , 24* (3).

Feraboli, P. (2006). Damage Resistance Characteristics of Thick-Core Honeycomb Composite Panels. *47th AIAA/ASME/ASCE/AHS/ASC Structures, Structural Dynamics, and Materials Conference.* Newport, Rhode Island.

Fu, J., Luo, H., Wang, W., & Wang, Z. (2017). Dynamic Response Analysis of Solar Array of a Satellite. *IEEE 3rd Information Technology and Mechatronics Engineering Conference (ITOEC).*

Gibson, L., & Ashby, M. (1997). *Cellular Solids : Structure and Properties, 2nd edition.* Cambridge: Cambridge University Press.

Grediac, M. (1993). A finite element study of the transverse shear in honeycomb cores. *International Journal of Solids and Structures , 30* (13), 1777-1788.

Hao, L., Geng, L., Shangjun, M., & Wenbin, L. (2011). Dynamic Analysis of the Spacecraft Structure on Orbit Made up of Honeycomb Sandwich Plates. *IEEE International Conference on Computer Science and Automation Engineering* . Shanghai.

HEXCEL-Composites. (1999). *HexWeb Honeycomb Attributes and Properties.* Hexcel Composites.

Hussain, M., Khan, R., & Abbas, N. (2018). Experimental and computational studies on honeycomb sandwich structures under static and fatigue bending load. *Journal of King Saud University–Science* .

Jiang, D., Zhang, D., Fei, Q., & Wu, S. (2014). An approach on identification of equivalent properties of honeycomb core using experimental modal data. *Finite Elements in Analysis and Design , 90*, 84–92.

Kelsey, S., Gellatly, R., & Clark, B. (1958). The shear modulus of foil honeycomb. *Aircraft Engineering and Aerospace Technology , 30* (10), 294-302.

Khan, M. K. (2006). Compressive and lamination strength of honeycomb sandwich panels with strain energy calculation from ASTM standards. *Journal of aerospace engineering , 220* (5), 375–386.

Kim, B., & Lee, D. L. (2010). Development of a satellite structure with the sandwich T-joint. *Composite Structures* , 460–468.

Kolopp, A., Rivallant, S., & Bouvet, C. (2013). Experimental study of sandwich structures as armour against medium-velocity impacts. *International Journal of Impact Engineering , 61*, 24-35.

Li, X., Li, K., Din, Y., Chen, R., & Lu, F. (2016). Inserting Stress Analysis of Combined Hexagonal Aluminum Honeycombs. *Shock and Vibration* .

Liu, Y., Gao, W., Liu, W., & Hua, Z. (2017). Numerical Analysis and Mechanical Properties of Nomex Honeycomb Core. *Proceedings of the ASME 2017 International Mechanical Engineering Congress and Exposition.* Tampa, Florida, USA.

Lv, L., Huang, Y., Cui, J., Qian, Y., Ye, F., & Zhao, Y. (2018). Bending properties of three-dimensional honeycomb sandwich structure composites. *Textile Research Journal , 88* (17), 2024-2031.

Olsen, T. (2010). *Electromechanical Materials Testing Machines.* USA.

Rodriguez-Ramirez, J., Castanie, B., & Bouvet, C. (2018). Experimental and numerical analysis of the shear nonlinear behaviour of Nomex honeycomb core. *Composite Structures , 193*, 121-139.

Roell, Z. *ProLine table-top testing machines Z010.* Germany.

Sorohan, Ş., Sandua, M., Sandua, A., & Constantinescu, D. M. (2015). Finite element models used to determine the equivalent in-plane properties of honeycombs. *DANUBIA ADRIA SYMPOSIUM on Advanced in Experimental Mechanics (DAS 2015).* ScienceDirect.

Su, P., Han, B., Zhao, Z., & Zhang, Q. (2018). Three-point bending of honeycomb sandwich beams with facesheet perforations. *Acta Mechanica Sinica , 34* (4), 667–675.

Sun, G., Huo, X., Chen, D., & Li, Q. (2017). Experimental and numerical study on honeycomb sandwich panels under bending and in-panel compression. *Materials & Design , 133*, 154-168.

Sun, W.-Q., & Cheng, W. (2017). Finite element model updating of honeycomb sandwich plates using a response surface model and global optimization technique. *Structural and Multidisciplinary Optimization* , 121–139.

Vinson, J. R. (2005). Sandwich Structures: Past, Present, and Future. *Sandwich Structures 7: Advancing with Sandwich Structures and Materials.* Springer, Dordrecht.

Xia, L.-j., Jin, X.-d., & Wang, Y.-b. (2001). The Equivalent Analysis of Honeycomb Sandwich Plates for Satellite Structure. *J Shanghai Jiao Tong Univ , 37* (7), 999-1001.

Zhang, T., Yan, Y., Li, J., & Luo, H. (2016). Low-velocity impact of honeycomb sandwich composite plates. *Journal of Reinforced Plastics and Composites , 35* (1), 8-32.